


CRITICAL REVIEW

Open Access



# Emerging role of 18F-FDG PET/CT in Castleman disease: a review

Benjamin Koa<sup>1,2†</sup>, Austin J. Borja<sup>1,3†</sup>, Mahmoud Aly<sup>1</sup>, Sayuri Padmanabhan<sup>1</sup>, Joseph Tran<sup>1</sup>, Vincent Zhang<sup>1</sup>, Chaitanya Rojulpote<sup>1</sup>, Sheila K. Pierson<sup>4</sup>, Mark-Avery Tamakloe<sup>4</sup>, Johnson S. Khor<sup>4</sup>, Thomas J. Werner<sup>1</sup>, David C. Fajgenbaum<sup>4</sup>, Abass Alavi<sup>1</sup> and Mona-Elisabeth Revheim<sup>1,5,6\*</sup> 

## Abstract

Castleman disease (CD) describes a group of rare hematologic conditions involving lymphadenopathy with characteristic histopathology and a spectrum of clinical abnormalities. CD is divided into localized or unicentric CD (UCD) and multicentric CD (MCD) by imaging. MCD is further divided based on etiological driver into human herpesvirus-8-associated MCD, POEMS-associated MCD, and idiopathic MCD. There is notable heterogeneity across MCD, but increased level of pro-inflammatory cytokines, particularly interleukin-6, is an established disease driver in a portion of patients. FDG-PET/CT can help determine UCD versus MCD, evaluate for neoplastic conditions that can mimic MCD clinico-pathologically, and monitor therapy responses. CD requires more robust characterization, earlier diagnosis, and an accurate tool for both monitoring and treatment response evaluation; FDG-PET/CT is particularly suited for this. Moving forward, future prospective studies should further characterize the use of FDG-PET/CT in CD and specifically explore the utility of global disease assessment and dual time point imaging.

*Trial registration* ClinicalTrials.gov, NCT02817997, Registered 29 June 2016, <https://clinicaltrials.gov/ct2/show/NCT02817997>

**Keywords:** Castleman disease, Positron emission tomography/computed tomography, Fluorodeoxyglucose F18, Interleukin-6, HIV

## Key Points

- Castleman disease (CD) describes a group of rare hematologic disorders involving lymphadenopathy with characteristic histopathology and a spectrum of clinical abnormalities.
- FDG-PET/CT allows detection of inflammation at a molecular level in CD that may precede structural changes detected by CT and MRI.
- FDG-PET/CT can contribute to correct sub-classification of CD into unicentric CD (UCD) and multicentric CD (MCD).

## Background

Castleman disease (CD), also known as angiofollicular lymph node hyperplasia and giant lymph node hyperplasia, is a hematologic disorder first reported by Benjamin Castleman in 1954. CD is a rare disease diagnosed in 6600–7700 individuals each year in the USA [1]. No data suggest a strong gender predilection [2]. All CD patients are present with lymphadenopathy that demonstrates characteristic histopathological changes and a spectrum of clinical abnormalities.

CD is sub-classified based on the number of enlarged lymph nodes. Unicentric CD (UCD) involves a single lymph node or a single region of nodes, while multicentric CD (MCD) involves multiple lymphatic stations [3]. Available data suggest that UCD is more common than MCD [1]. UCD has been reported to occur in younger individuals than MCD, though epidemiologic data are

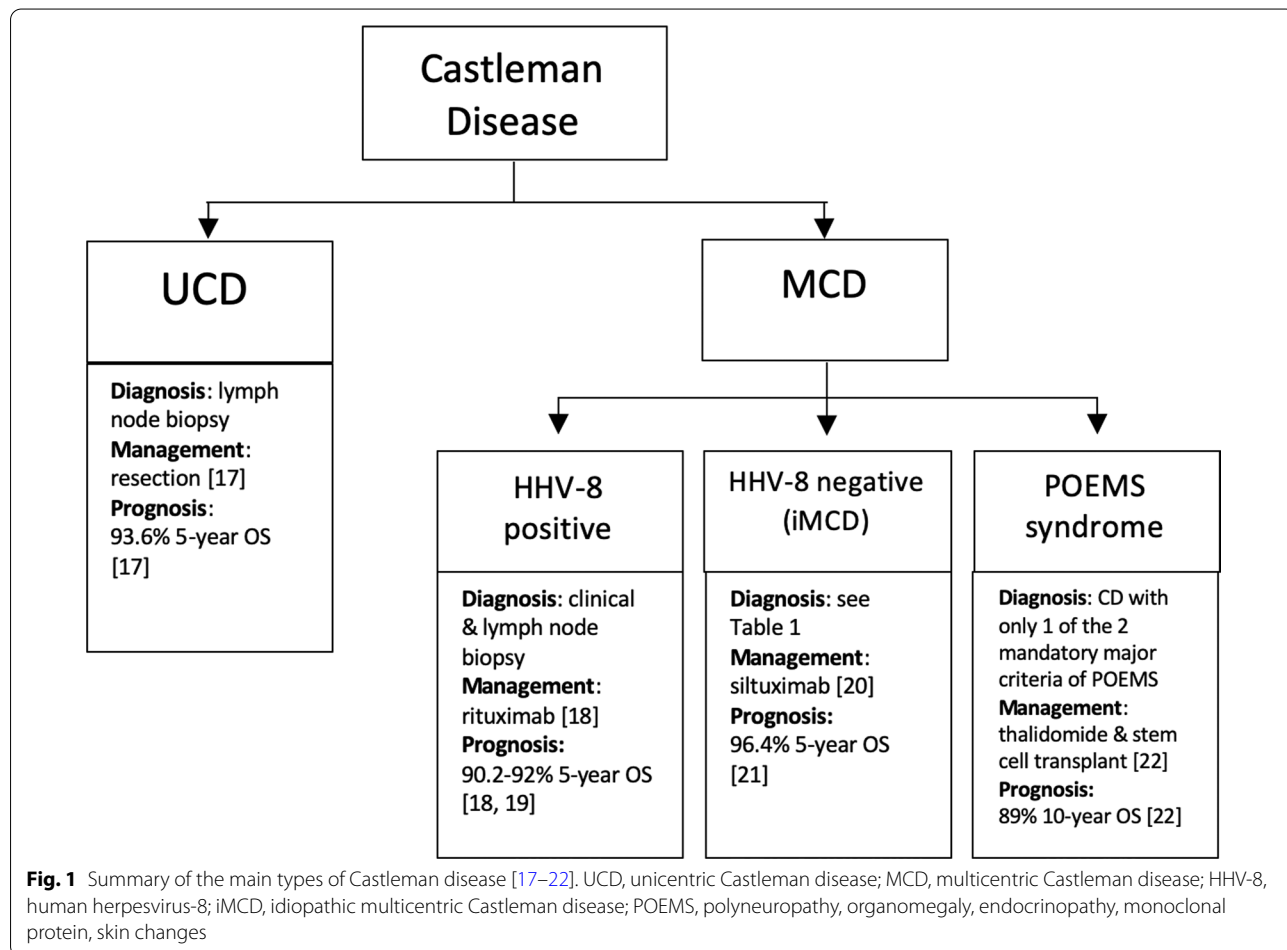
\*Correspondence: mona.elisabeth.revheim@ous-hf.no

<sup>†</sup>Benjamin Koa and Austin J. Borja represent co-first authorship. Full list of author information is available at the end of the article

sparse, and both can occur in individuals of all ages [4, 5]. Most cases of UCD are located in the mediastinum, but UCD can involve any lymph node region in the body [6–9]. In contrast, MCD involves lymphadenopathy in greater than one region and can occur in any region of the body. Additionally, MCD has a poorer prognosis than UCD. MCD is further divided into three subgroups: human herpesvirus 8 (HHV-8)-associated MCD; polyneuropathy, organomegaly, endocrinopathy, monoclonal gammopathy, skin changes (POEMS)-associated MCD; and idiopathic MCD (iMCD) [10]. The relative breakdown between HHV-8-associated MCD, POEMS-associated MCD, and iMCD is not well characterized. These four groups vary considerably in clinical characteristics, preferred treatment, and clinical outcomes. Therefore, correct classification is vital at the time of diagnosis. In addition, many diseases are present with CD-like clinicopathology, including lymphoma, Kaposi sarcoma, immunoglobulin G4-related disease (IgG4-RD), and other benign and malignant tumors [11–14]. Furthermore, HHV-8-associated MCD is often seen in human

immunodeficiency virus (HIV)-positive or otherwise immunosuppressed patients who are at increased risk for such CD-like diseases [4, 15, 16]. As such, the exclusion of pathologies that can mimic CD is critical. The features, prognosis, and management of each main subtypes of CD are summarized in Fig. 1 [17–22].

The standard investigative workup in Castleman disease usually begins with lymph node biopsy followed by radiological investigation with PET/CT preferred, complete blood count, serum chemistry, markers of inflammation, serum cytokine levels, viral serology for HHV-8 and HIV, and protein electrophoresis, immunofixation, and quantitative immunoglobulins [23]. To further exclude other similarly presenting conditions, clinical findings must be considered and other laboratories can be ordered such as IgH gene arrangement study on the biopsied lymph node to rule out lymphoma and serology investigations for autoimmune disorders [23]. A formal diagnostic criteria have only been established for iMCD and are summarized in Table 1 [4]. Diagnosis of HHV-8 associated MCD generally requires HHV-8 detection,



lymphadenopathy in multiple regions, and plasmablastic histopathologic findings on lymph node biopsy [24]. POEMS-associated MCD is diagnosed if only one of two the mandatory major criteria of polyneuropathy and monoclonal plasma proliferative disorder needed for diagnosis of POEMS syndrome is present with lymph node biopsy diagnostic of CD [25].

Excessive cytokine production is believed to underlie CD pathogenesis. UCD and POEMS-associated MCD are believed to be caused by somatic mutations in monoclonal stromal and plasma cells, respectively, resulting in excessive cytokine release and subsequent clinical symptomatology [26]. In HHV-8-associated MCD, uncontrolled infection with HHV-8 occurs due to host immunocompromise, leads to a viral interleukin (IL)-6 driven cytokine storm, and correlates with symptom severity [27–30]. Finally, while the precise mechanism of iMCD is not known, elevated IL-6 associated with autoimmune mechanisms, ectopic cytokine secretion by tumor cells, and/or viral signaling by a non-HHV-8 virus have been proposed as possible etiologies [15]. IL-6 levels directly parallel disease activity, and elevated serum IL-6 induces B-lymphocyte growth, secretion of vascular

endothelial growth factor (VEGF), and inflammatory responses. Also, mice with retroviral transduction of IL-6 coding sequence within hematopoietic stem cells develop an MCD-like syndrome [31]. As we discuss in the following sections, the modulation of IL-6 and other inflammatory cytokines is effective in a large portion of iMCD patients.

### Common presenting symptoms and laboratory abnormalities in CD

UCD may be clinically silent, and recent evidence suggests that most UCD patients do not demonstrate any signs or symptoms beyond solitary lymphadenopathy [32]. That being said, UCD may predispose patients to malignancy [33, 34]. Laboratory findings, including complete blood count and inflammatory markers, are typically unremarkable in UCD patients.

In contrast, the three subtypes of MCD (HHV-8-associated MCD, POEMS-associated MCD, iMCD) present with diffuse lymphadenopathy, systemic inflammation, and organ dysfunction. These patients typically demonstrate B symptoms (fever, chills, night sweats), cough,

**Table 1 From the iMCD consensus diagnostic criteria proposed from The International Working Group for iMCD [4]**

#### Major criteria

1. Lymph nodes with histopathologic features consistent with iMCD spectrum
2. Enlarged lymph nodes ( $\geq 1$  cm in short-axis diameter) in  $\geq 2$  lymph node regions

#### Minor criteria

##### Laboratory

1. Elevated CRP or ESR
2. Anemia
3. Thrombocytopenia or thrombocytosis
4. Hypoalbuminemia
5. Renal dysfunction or proteinuria
6. Polyclonal hypergammaglobulinemia

##### Clinical

1. B symptoms
2. Hepatomegaly or splenomegaly
3. Fluid accumulation
4. Eruptive cherry hemangiomas
5. Violaceous papules
6. Lymphocytic interstitial pneumonitis

#### Supporting features

1. Elevated IL-6, VEGF, IgA, IgE, LDH, and/or B2M
2. Reticulin fibrosis of bone marrow
3. Disorders associated with iMCD: paraneoplastic pemphigus, bronchiolitis obliterans organizing pneumonia, autoimmune cytopenias, polyneuropathy, inflammatory myofibroblastic tumor

#### Exclusion criteria

1. Infection: HHV-8, EBV, CMV, toxoplasmosis, HIV, active tuberculosis
2. Autoimmune/autoinflammatory: systemic lupus erythematosus, rheumatoid arthritis, adult-onset Still disease, juvenile idiopathic arthritis, autoimmune lymphoproliferative syndrome
3. Malignancy: lymphoma, multiple myeloma, POEMS syndrome, primary lymph node plasmacytoma, follicular dendritic cell sarcoma

\* Diagnosis requires both major criteria and at least 2 of 11 minor criteria with 1 laboratory criterion. Diseases that can mimic iMCD listed in the exclusion criteria must be ruled out

iMCD, idiopathic Castleman disease; CRP, C-reactive protein; ESR, erythrocyte sedimentation rate; IL-6, interleukin 6; VEGF, vascular endothelial growth factor; IgA, immunoglobulin A; IgE, immunoglobulin E; LDH, lactate dehydrogenase; B2M, Beta-2 microglobulin; HHV-8, human herpesvirus-8; EBV, Epstein-Barr virus; CMV, cytomegalovirus; POEMS, polyneuropathy, organomegaly, endocrinopathy, monoclonal protein, skin changes)

thoracic or abdominal pain, dyspnea, weight loss, and hemoptysis [32]. Comorbid malignancies, including lymphoma in iMCD and Kaposi's sarcoma in HHV-8-associated MCD, have been found to occur [31, 33, 34]. In addition, patients with the three subtypes of MCD may demonstrate numerous laboratory abnormalities, including anemia, leukocytosis, thrombocytopenia and thrombocytosis, elevated inflammatory markers (C-reactive protein, IL-6, and erythrocyte sedimentation rates), elevated IgG, hypoalbuminemia, renal dysfunction, and elevated liver enzymes [1, 31]. Of note, serological tests for hepatitis B virus, cryoglobulin, antinuclear antibody, and cytomegalovirus are usually negative [35]. Consensus diagnostic criteria exist for iMCD and for POEMS syndrome, which should both be evaluated in all potential MCD cases. The heterogeneity of CD presents a challenge, so both clinical and laboratory findings must be carefully considered in the diagnosis and workup for suspected CD [4, 25].

### Role of FDG-PET/CT in the diagnosis of CD

<sup>18</sup>F-fluorodeoxyglucose-positron emission tomography/computed tomography (FDG-PET/CT) can be used to assess the metabolic activity of the enlarged lymph nodes in CD. FDG is a radiolabeled glucose analog taken up preferentially by metabolically active cells, such as malignant tumor cells or inflammatory cells [9]. Currently, FDG-PET/CT is recommended as an alternative to CT scan alone in the published iMCD treatment guidelines [36]. However, the potential for FDG-PET/CT in the diagnosis, treatment assessment, and follow-up of CD has not been fully demonstrated. With the ability to collect structural and metabolic information, FDG-PET/CT can enhance the specificity and sensitivity in identifying affected lymph nodes in CD patients [11]. Specifically, contrast-enhanced PET/CT would provide joint functionality of both contrast-enhanced CT and PET.

Currently, CT is routinely utilized in CD patients to identify and characterize lymph nodes by size, shape, and contrast enhancement pattern [7]. The lymphadenopathy in UCD, HHV-8-associated MCD, POEMS-associated MCD, and iMCD typically demonstrates marked and rapid contrast enhancement on CT [37]. HHV-8-associated MCD, POEMS-associated MCD, and iMCD may

additionally present with hepatosplenomegaly and other organ-specific imaging anomalies. Of note, thickening of the lung septa, bronchovascular bundles, and centrilobular nodules may present on CT as thin-walled cysts and ground-glass opacity [8, 9, 13].

A major limitation of CT is that it cannot sensitively detect the involvement of normal-sized lymph nodes, nor can it distinguish between reactive hyperplasia and pathological enlargement of lymph nodes. Additionally, CD can sometimes be misinterpreted via CT and magnetic resonance imaging (MRI) as other similarly appearing autoimmune, malignant, or infectious disorders [3, 4, 11, 14] (Table 2). For example, thoracic UCD may be interpreted as a thyroid mass, parathyroid adenoma, or hemangiomas [9].

Fused FDG-PET/CT takes into account the metabolic characteristics of the structures [38]. This molecular imaging modality, thus, can detect abnormally high uptake in small lymph nodes that would be overlooked by purely structural imaging modalities and facilitate a correct and complete diagnosis. Also, FDG-PET/CT can identify lymph nodes and lesions that are more likely to yield a definitive diagnosis on biopsy [39]. Even in cases of UCD with only mild contrast enhancement on CT, focal lymphadenopathy can demonstrate increased FDG uptake. The majority of HHV-8-associated MCD patients also show increased FDG uptake in the bone marrow and the spleen [39]. In addition, lung parenchymal changes in iMCD may be confirmed by increased FDG uptake. That being said, many institutions may not implement breath-holds for the pulmonary portion of the scans, potentially obscuring fine details of the lung parenchyma and leading to less accurate longitudinal measurement of small lung lesions due to respiratory motion artifact [40, 41]. In these cases, additional techniques to correct for respiratory motion artifacts, such as phase-aligned correction and gating algorithms, are warranted [42, 43].

The degree of FDG uptake may be different between UCD, HHV-8-associated MCD, POEMS-associated MCD, and iMCD. While one study reported a significantly higher lymph nodes maximum standardized uptake value (SUV<sub>max</sub>) in MCD versus UCD, another study noted no significant difference [44, 45]. Clinical manifestations of CD have also been shown to be

**Table 2 Autoimmune, neoplastic, and infectious disorders with significant shared clinical, histologic, and immunologic features of Castleman disease (CD) [3, 4, 11, 14]**

Types of disorders	Disorders
Autoimmune	Immunoglobulin G4-related disease, rheumatoid arthritis (RA), systemic lupus erythematosus (SLE), adult-onset Still Disease
Neoplastic	Lymphoma, desmoid tumors, retroperitoneal sarcoma, paragangliomas, sarcomas, hemangiopericytoma, bronchial adenoma, neurofibroma, chest wall tumors, schwannoma
Infectious	Human immunodeficiency Virus (HIV), Epstein–Barr virus (EBV), cytomegalovirus, tuberculosis, toxoplasmosis

correlated with the degree of FDG uptake in a small study [38]. However, the use of SUV as the sole means of differentiation between subtypes has significant limitations. SUV is specific to the technique and instrumentation used, which is highly variable among institutions [46, 47]. Nevertheless, PET/CT scanners and the imaging protocol adhered are increasingly standardized to international practice guidelines and the PET/CT systems including calibration and harmonized to a phantom reduce the variation of quantitation parameters [48, 49].

Although some evidence indicates that FDG-PET/CT may be utilized to differentiate between CD subtypes, as well as between CD and lymphoma as potential causes of lymphadenopathy, additional studies must be performed to corroborate these findings [34, 45, 50–52]. In addition, MCD patients are at increased risk for the development of lymphoma, which can confound FDG uptake findings [53]. A potential confounder for the use of FDG in the evaluation of lymphadenopathy is sarcoidosis, which can resemble lymphoma and CD both morphologically and metabolically, and may rarely coexist with CD [54]. Laboratory findings may help differentiate other inflammatory conditions from CD; however, histopathological evaluation through tissue biopsy is the recommended approach in evaluating unexplained lymphadenopathy [55].

Although excisional lymph node biopsy is the only way to definitively diagnose CD based on its histology, existing evidence suggests that FDG-PET/CT should be performed beforehand to help determine CD subtype, consider the possibility of lymphoma, and identify ideal lesions for biopsy [39, 45].

### **FDG-PET/CT in treatment assessment and monitoring of CD**

Treatment options for CD and responses differ by subtype. For UCD, complete surgical resection of the node is an effective and usually curative treatment. When complete surgical excision cannot be performed, chemotherapy and radiation therapy are alternative therapies that sometimes can be followed by resection [56, 57].

The first-line treatment for HHV-8-associated MCD involves rituximab, an anti-CD20 monoclonal antibody, with or without antivirals and liposomal doxorubicin. Treatment of POEMS-associated MCD is directed against the underlying POEMS syndrome using immunomodulators and autologous stem cell transplantation. iMCD is treated first-line with the anti-IL-6 immunotherapy siltuximab (the only FDA-approved treatment for iMCD), which may be combined with corticosteroids. iMCD refractory to siltuximab may be treated with rituximab, immunosuppressants (e.g., sirolimus, cyclosporine), immunomodulators (e.g., thalidomide, bortezomib), or multi-agent cytotoxic chemotherapy for

severe disease [58]. With more insight into disease mechanisms and signal pathways involved in iMCD, new treatment strategies are under investigation.

Beyond identifying lymphadenopathy, FDG-PET/CT can be utilized to monitor response to treatment [39, 59]. One report on CD used FDG-PET/CT to confirm a complete anatomic and metabolic response to treatment and to enable early detection of treatment failure or relapse [60] (Figs. 2, 3).

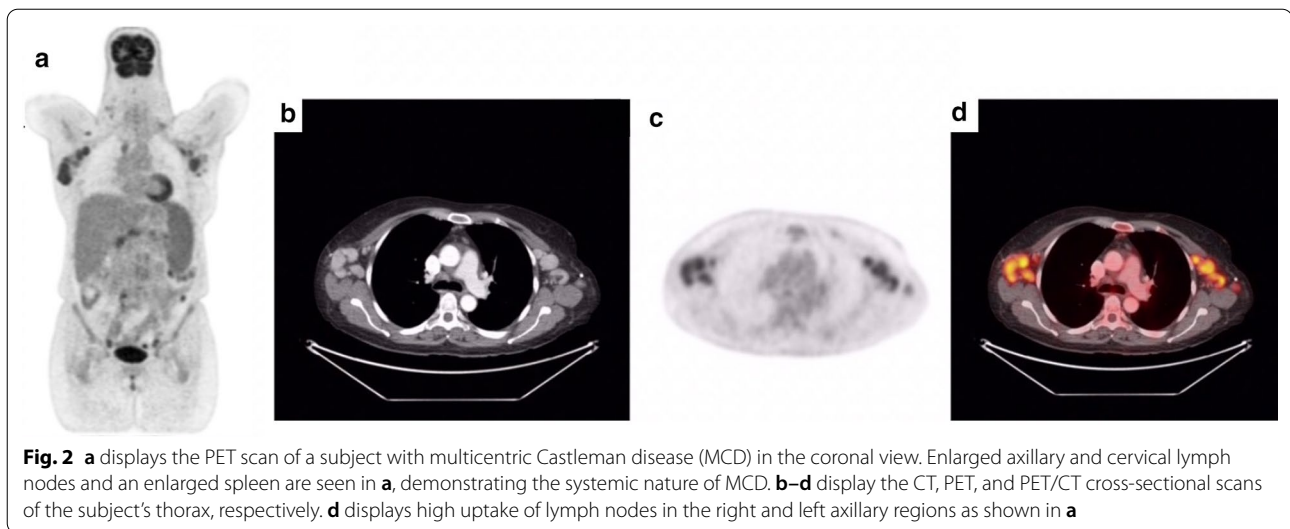
The relapse of UCD after surgery is rare, and only a few cases have been reported [61, 62]. In contrast, HHV-8-associated MCD, POEMS-associated MCD, and iMCD frequently relapse [18, 63]. In particular, iMCD is a heterogeneous disease and not all iMCD patients respond to treatment, including anti-IL-6 therapies. The only published treatment guidelines for iMCD recommend follow-up imaging by CT or PET/CT [64]. Therefore, the role of FDG-PET/CT as both a prognostic and a monitoring tool should be further investigated.

Following rituximab therapy in HIV-positive patients with HHV-8-associated MCD, the median time to the first MCD relapse was 30 months [18]. In addition, clinicopathological features present at diagnosis have been associated with subsequent relapse [18]. In HHV-8-associated MCD, patients often have comorbid HIV infection, so the interpretation of FDG-PET/CT can be confounded by reactive changes secondary to viremia, concurrent infections, or lipodystrophy [39]. Other malignancies and inflammatory diseases may further complicate the monitoring of CD [65, 66]. Consequently, FDG-PET/CT should be interpreted together with clinical and laboratory information in the monitoring of disease activity in HHV-8-associated MCD, POEMS-associated MCD, and iMCD [67].

### **Future perspectives: dual time-point (DTP) imaging and global disease assessment**

Although FDG-PET/CT is effective in detecting and monitoring CD, some limitations and challenges are evident. Most significantly increased FDG uptake is not specific to CD, and several other disorders can mimic CD. As such, two nascent FDG-PET/CT techniques may prove to be useful in the assessment of CD: dual time-point FDG-PET imaging (DTP) and global disease score (GDS).

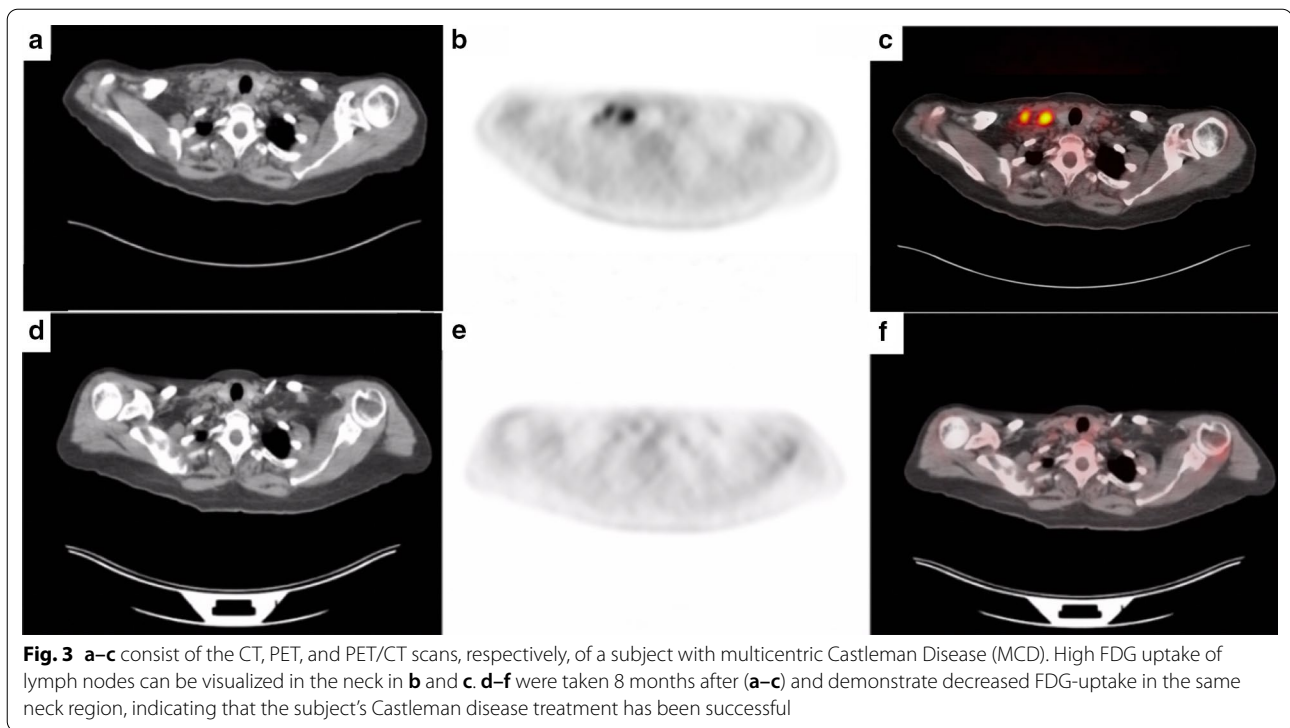
DTP involves an extra acquisition of PET data at a delayed time-point (e.g., 3 h or more after FDG administration). Most cancers demonstrate maximum FDG uptake well beyond 60 min after FDG administration, while normal tissues and inflammatory lesions generally show a decline in FDG uptake with time. Thus, DTP imaging has been demonstrated improve discrimination between cancer and inflammatory lesions [68–70]. DTP



also provides additional information on disease biology [71]. Different types of malignant and inflammatory cells accumulate variable amounts of FDG due to variation in glucose-6-phosphatase. More aggressive and actively proliferating cancer cells express lower levels of glucose-6-phosphatase and exhibit rising levels of FDG uptake over a longer period, whereas the opposite is applicable in less aggressive or less proliferative cancer cells and inflammatory cells [68]. Hence, differential kinetics of FDG uptake and clearance from inflammatory and tumor cells over time may allow us to distinguish between malignancy and inflammation. Moreover, acute infectious and non-infectious inflammatory lesions behave differently from chronic lesions on delayed time-point imaging due to the different inflammatory cells involved. However, this methodology can be demanding to both implement and standardize within busy imaging departments [72]. In addition, clinician experience in interpreting morphological features on imaging is strongly related to ability to differentiate malignancy from inflammatory mimics. For these reasons, we propose that this technique be expanded to include CD. Specifically, CD tends to demonstrate a symmetric pattern in the mediastinum and hilum [9]. The performance of qualitative over quantitative metrics in inflammatory conditions has also gained some recent interest [73]. Nonetheless, a more thorough exploration of DTP is needed to assess its efficacy in differentiating between patterns of FDG uptake and clearance in active (acute) versus inactive (chronic) inflammatory lesions in CD, which could potentially help

detect acute episodes of exacerbation and monitor the underlying chronic inflammatory state of CD.

Although CT with intravenous contrast may help with the localization of CD lesion, it cannot be used to quantify lesional activity or track it longitudinally. FDG-PET/CT imaging has been utilized in a number of other pathologies to calculate global disease burden, which uses GDS metrics including total lesion glycolysis (TLG). TLG represents a volumetric measure of FDG uptake by multiplying metabolic lesion volume (MLV) and SUVmean values obtained by using a threshold to delineate lesion activity relative to the background [74]. Single SUVmax measurements are often unreliable and unreproducible, especially when glucose uptake is heterogeneous and the disease is systemic with multiple lesions; TLG, on the other hand, is a sensitive and specific value that gives insight into the stage and progression of a disease [75–77] (Figs. 4, 5). Global disease assessment could potentially make this method of tracking disease over time of treatment easy and standardized. That is, GDS reflects the total disease burden and metabolic activity at the time of the PET examination and can be followed longitudinally to monitor disease activity and treatment efficacy [46]. This methodology has previously been applied to lymphoma patients [78–80]. Moving forward, an analogous approach should be applied toward MCD patients, especially iMCD. Despite the effectiveness and an increased use of this methodology, it has still not been widely adopted and standardized in all institutions. Nevertheless, we believe that GDS will better



track the progress CD, especially given its heterogeneous presentation.

Beyond this, GDS may be used to standardize the assessment of CD progression among individuals and to monitor response to novel therapies currently under investigation [81–83]. A recent study demonstrated that IL-6-blockade refractory iMCD is responsive to sirolimus, a mammalian target of rapamycin (mTOR) inhibitor [58]. FDG-PET/CT is excellent in the early evaluation of signal transduction inhibitors like mTOR inhibitors for multiple other conditions as FDG-PET/CT detects early changes in tumor biology preceding tumor size regression, and treatment effects can be detected as early as 24 h after onset of treatment [84–87]. Therefore, FDG-PET/CT has the potential to become a powerful tool for future evaluation of biologic agents and other therapies for CD.

## Conclusion

CD is a potentially fatal disease that may overlap with numerous hematologic, inflammatory, and neoplastic diseases. FDG-PET/CT is frequently performed to visualize and localize lymph node enlargement in CD, but it has not been systematically applied in clinical practice. In the future, we believe that FDG-PET/CT and associated techniques will be useful in the diagnosis and categorization of CD, in differentiation between mimicking conditions, and monitoring of disease progression and response to treatment. Future prospective studies should be designed to assess and validate the role of this molecular imaging modality to aid in the characterization and management of this rare orphan disease.

## Abbreviations

CD: Castleman disease; DTP: Dual time-point FDG-PET imaging; FDG-PET/CT: 18F-fluorodeoxyglucose-positron emission tomography/computed tomography; MRI: Magnetic resonance imaging; GDS: Global disease score;

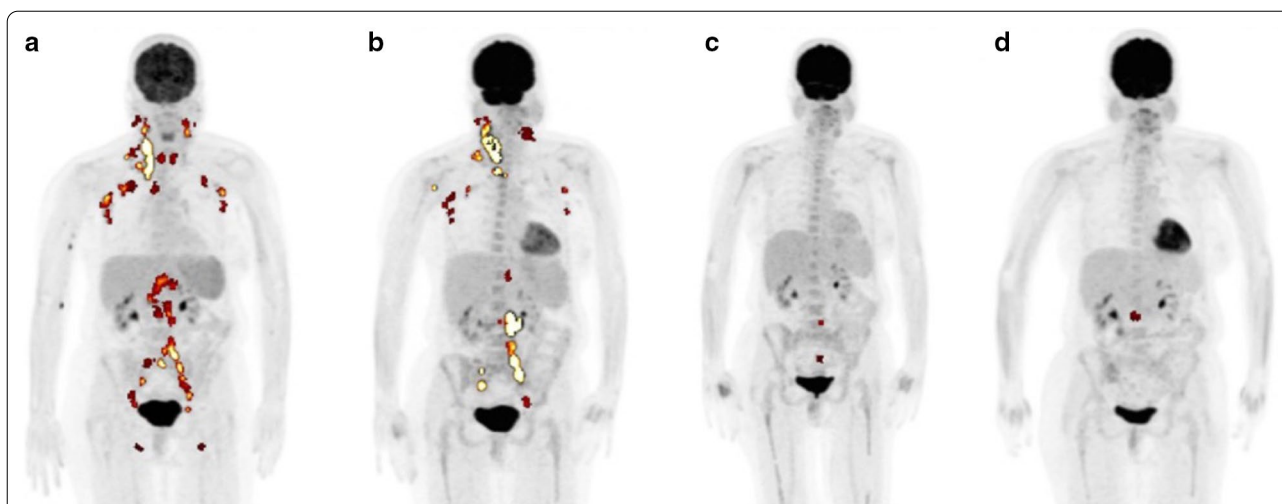


**Fig. 4** FDG-PET images of a multicentric Castleman disease (MCD) subject over 8 months. **a** and **b** demonstrate cervical, axillary, and pelvic lesions, while **c** and **d** show decrease in FDG-uptake in accordance to treatment. Total lesion glycolysis (TLG) was calculated to be 934.7, 1001.7, 17.5, and 16.4 for **a–d** respectively. TLG was calculated by multiplying the metabolic volume with FDG uptake segmented by fixed threshold methods at 41% of maximum SUV in the volume of interest (VOI) [75] by the mean standardized uptake value (SUVmean) and then summing all the intensity-volume product values from all lesions

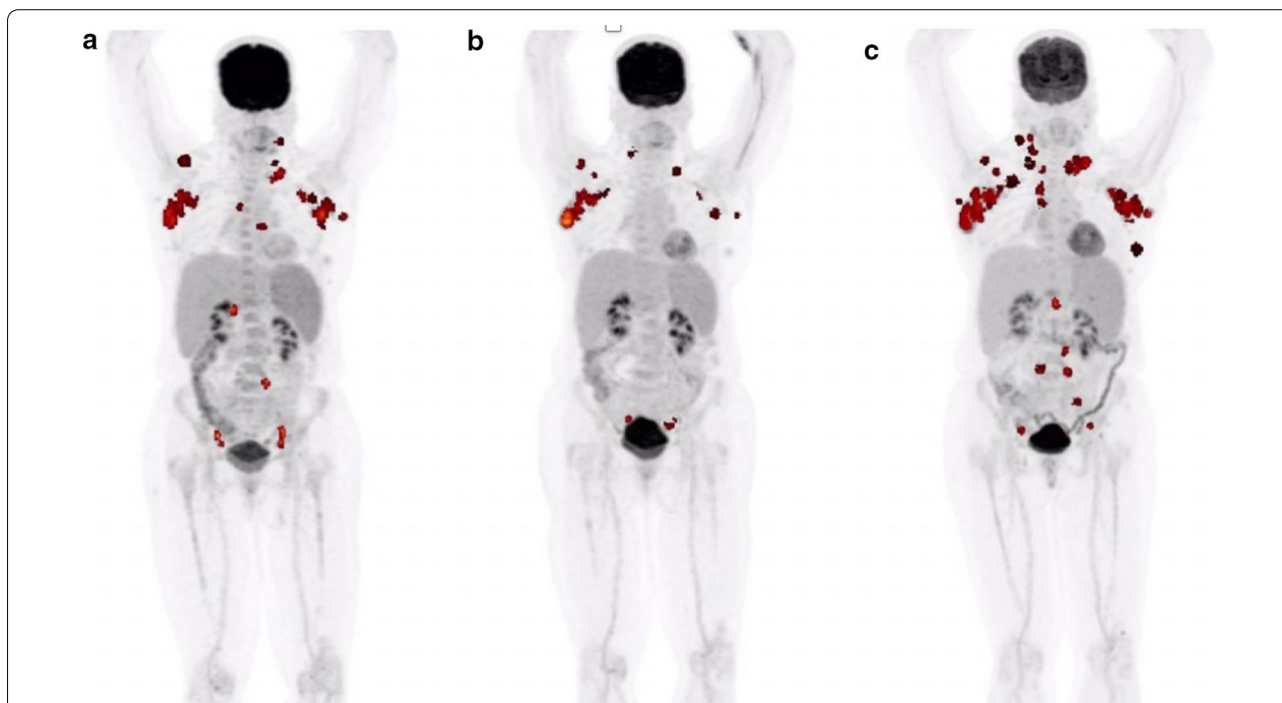


**Fig. 5** A subject with multicentric Castleman disease (MCD) with lesions in the axillary, neck, and abdomen is shown over the course of 10 months. **a** indicated the initial lesions seen in PET before treatment. **b** was taken after 4 months from the initial scan, and a decrease of lesions in the axillary, neck, and abdomen is seen. However, the disease seemed to reappear in the axillary and cervical lesions despite treatment as visualized in **c**, which was taken 6 months after the scan for **b**. Total lesion glycolysis (TLG) was calculated to be 365.9, 204.5, and 601.6 for **a–c**, respectively. TLG was calculated by multiplying the metabolic volume with FDG uptake segmented by fixed threshold methods at 41% of maximum SUV in the volume of interest (VOI) [75] by the mean standardized uptake value (SUVmean) and then summing all the intensity-volume product values from all lesions



HHV-8: Human herpesvirus-8; HIV: Human immunodeficiency virus; IgG4-RD: Immunoglobulin G4-related disease; IL: Interleukin; iMCD: Idiopathic MCD; MCD: Multicentric CD; mTOR: Mammalian target of rapamycin; MTV: Metabolic tumor volume; POEMS: Polyneuropathy, organomegaly, endocrinopathy, monoclonal gammopathy, skin changes; SUV: Standardized uptake value; SUVmax: Maximum SUV; SUVmean: Mean SUV; TLG: Total lesion glycolysis; UCD: Unicentric CD; VEGF: Vascular endothelial growth factor.

#### Acknowledgements

We would like to thank all of the CD patients who volunteered for our studies.

#### Authors' contributions

BK analyzed the patient data and was a major contributor in writing the manuscript. AB was a major contributor in writing the manuscript. MA substantially analyzed and interpreted the patient data. SP substantially analyzed and was a contributor in writing of the manuscript. JT made considerable contributions to the drafting of the manuscript. VZ was a contributor to the drafting and revision of the manuscript. CR made considerable contributions to the drafting of the manuscript. SKP contributed to the conception and acquisition of the project and was a contributor to the writing of the manuscript. MAT was a substantial contributor to the writing and revision of the manuscript. JST was a substantial contributor to the writing and revision of the manuscript. TJW made substantial contributions to the acquisition of the patient data and design of the project. DCF was a major contributor to the conception of the project, design of the work, and writing of the manuscript. AA was a major contributor to the conception of the project and writing of the manuscript. MR was a major contributor to the writing and revision of the manuscript. All authors read and approved the final manuscript and have agreed to be personally accountable for the author's own contributions.

#### Funding

DCF has received research funding from EUSA Pharma for the ACCELERATE Registry (formerly sponsored by Janssen Pharmaceuticals).

#### Availability of data and materials

The datasets used and/or analyzed during the current study are available from the corresponding author on reasonable request.

#### Competing interests

DCF has received research funding from EUSA Pharma for the ACCELERATE Registry (formerly sponsored by Janssen Pharmaceuticals). The rest of the authors declare no conflicts of interest.

#### Ethical approval

Clinical Trial ID: NCT02817997. All procedures performed in studies involving human participants were in accordance with the ethical standards of the institutional and/or national research committee and with the 1964 Declaration of Helsinki and its later amendments or comparable ethical standards.

#### Consent for publication

Not applicable.

#### Author details

<sup>1</sup> Department of Radiology, University of Pennsylvania, Philadelphia, PA, USA. <sup>2</sup> Drexel University College of Medicine, Philadelphia, PA, USA. <sup>3</sup> Perelman School of Medicine at the University of Pennsylvania, Philadelphia, PA, USA. <sup>4</sup> Department of Medicine, Division of Translational Medicine and Human Genetics, University of Pennsylvania, Philadelphia, PA, USA. <sup>5</sup> Division of Radiology and Nuclear Medicine, Oslo University Hospital, Sognsvannsveien 20, 0372 Oslo, Norway. <sup>6</sup> Institute of Clinical Medicine, Faculty of Medicine, University of Oslo, Problemveien 7, 0316 Oslo, Norway.

Received: 1 November 2020 Accepted: 4 January 2021

Published online: 11 March 2021

#### References

- Munshi N, Mehra M, van de Velde H, Desai A, Potluri R, Vermeulen J (2015) Use of a claims database to characterize and estimate the incidence rate for Castleman disease. *Leuk Lymphoma* 56:1252–1260

- Cervantes CE, Correa R (2015) Castleman disease: a rare condition with endocrine manifestations. *Cureus* 7:e380
- Bonekamp D, Horton KM, Hruban RH, Fishman EK (2011) Castleman disease: the great mimic. *Radiographics* 31:1793–1807
- Fajgenbaum DC, Uldrick TS, Bagg A et al (2017) International, evidence-based consensus diagnostic criteria for HHV-8-negative/idiopathic multicentric Castleman disease. *Blood* 129:1646–1657
- Jiang J-P, Shen X-F, Du J-F, Guan W-X (2018) A retrospective study of 34 patients with unicentric and multicentric Castleman's disease: experience from a single institution. *Oncol Lett* 15:2407–2412
- Yu JY, Oh IJ, Kim KS et al (2014) Castleman's disease presenting as a tracheal mass. *Ann Thorac Surg* 97:1798–1800
- Ye B, Gao S-G, Li W et al (2010) A retrospective study of unicentric and multicentric Castleman's disease: a report of 52 patients. *Med Oncol* 27:1171–1178
- Luo JM, Li S, Huang H et al (2015) Clinical spectrum of intrathoracic Castleman disease: a retrospective analysis of 48 cases in a single Chinese hospital. *BMC Pulm Med* 15:34
- Kligerman SJ, Auerbach A, Franks TJ, Galvin JR (2016) Castleman disease of the thorax: clinical, radiologic, and pathologic correlation: from the radiologic pathology archives. *Radiographics* 36:1309–1332
- Cronin DMP, Warnke RA (2009) Castleman disease: an update on classification and the spectrum of associated lesions. *Adv Anat Pathol* 16:236
- Madan R, Chen JH, Trotman-Dickenson B, Jacobson F, Hunsaker A (2012) The spectrum of Castleman's diseases: Mimics, radiologic pathologic correlation and role of imaging in patient management. *Eur J Radiol* 81:123–131
- Delaney SW, Zhou S, Maceri D (2015) Castleman's disease presenting as a parotid mass in the pediatric population: a report of 2 cases. *Case Rep Otolaryngol* 2015:691701
- Oksenhendler E, Boutboul D, Fajgenbaum D et al (2018) The full spectrum of Castleman disease: 273 patients studied over 20 years. *Br J Haematol* 180:206–216
- Chen LYC, Mattman A, Seidman MA, Carruthers MN (2019) IgG4-related disease: what a hematologist needs to know. *Haematologica* 104:444–455
- Fajgenbaum DC, van Rhee F, Nabel CS (2014) HHV-8-negative, idiopathic multicentric Castleman disease: novel insights into biology, pathogenesis, and therapy. *Blood* 123:2924–2933
- Powles T, Stebbing J, Bazeos A et al (2009) The role of immune suppression and HHV-8 in the increasing incidence of HIV-associated multicentric Castleman's disease. *Ann Oncol* 20:775–779
- Zhang X, Rao H, Xu X et al (2018) Clinical characteristics and outcomes of Castleman disease: a multicenter study of 185 Chinese patients. *Cancer Sci* 109:199–206
- Pria AD, Pinato D, Roe J, Naresh K, Nelson M, Bower M (2017) Relapse of HHV8-positive multicentric Castleman disease following rituximab-based therapy in HIV-positive patients. *Blood* 129:2143–2147
- Gérard L, Michot J-M, Burcheri S et al (2012) Rituximab decreases the risk of lymphoma in patients with HIV-associated multicentric Castleman disease. *Blood Am Soc Hematol* 119:2228–2233
- Yu L, Tu M, Cortes J et al (2017) Clinical and pathological characteristics of HIV- and HHV-8-negative Castleman disease. *Blood* 129:1658–1668
- Sitenga J, Aird G, Ahmed A, Silberstein PT (2018) Impact of siltuximab on patient-related outcomes in multicentric Castleman's disease. *Patient Relat Outcome Meas* 9:35–41
- Suichi T, Misawa S, Sekiguchi Y et al (2020) Treatment response and prognosis of POEMS syndrome coexisting with Castleman disease. *J Neurol Sci* 413:116771
- Szalat R, Munshi NC (2018) Diagnosis of Castleman disease. *Hematol Oncol Clin North Am* 32:53–64
- Múzes G, Sipos F, Csomor J, Sréter L (2013) Multicentric Castleman's disease: a challenging diagnosis. *Pathol Oncol Res* 19:345–351
- Dispenzieri A (2019) POEMS syndrome: 2019 update on diagnosis, risk-stratification, and management. *Am J Hematol* 94:812–827
- Li Z, Lan X, Li C et al (2019) Recurrent PDGFRB mutations in unicentric Castleman disease. *Leukemia* 33:1035–1038
- van Rhee F, Stone K, Szmania S, Barlogie B, Singh Z (2010) Castleman disease in the 21st century: an update on diagnosis, assessment, and therapy. *Clin Adv Hematol Oncol* 8:486–498

28. Polizzotto MN, Ulrick TS, Wang V et al (2013) Human and viral interleukin-6 and other cytokines in Kaposi sarcoma herpesvirus-associated multicentric Castlemans disease. *Blood* 122:4189–4198
29. Suthaus J, Stuhlmann-Laeisz C, Tompkins VS et al (2012) HHV-8-encoded viral IL-6 collaborates with mouse IL-6 in the development of multicentric Castlemans disease in mice. *Blood* 119:5173–5181
30. Stebbing J, Pantanowitz L, Dayyani F, Sullivan RJ, Bower M, Dezube BJ (2008) HIV-associated multicentric Castlemans disease. *Am J Hematol* 83:498–503
31. El-Osta HE, Kurzrock R (2011) Castlemans disease: from basic mechanisms to molecular therapeutics. *Oncologist* 16:497–511
32. Zhao S, Wan Y, Huang Z, Song B, Yu J (2019) Imaging and clinical features of Castlemans disease. *Cancer Imaging* 19:53
33. Waterston A, Bower M (2004) Fifty years of multicentric Castlemans disease. *Acta Oncol* 43:698–704
34. Hill AJ, Tirumani SH, Rosenthal MH et al (2015) Multimodality imaging and clinical features in Castlemans disease: single institute experience in 30 patients. *Br J Radiol* 88:20140670
35. Savelli G, Muni A, Falchi R, Giuffrida F (2015) Pre- and post-therapy 18F-FDG PET/CT of a patient affected by non-HIV multicentric IgG4-related Castlemans disease. *Blood Res* 50:260–262
36. van Rhee F, Voorhees P, Dispenzieri A et al (2018) International, evidence-based consensus treatment guidelines for idiopathic multicentric Castlemans disease. *Blood* 132:2115–2124
37. Kwon S, Lee KS, Ahn S, Song I, Kim TS (2013) Thoracic Castlemans disease: computed tomography and clinical findings. *J Comput Assist Tomogr* 37:1–8
38. Lee ES, Paeng JC, Park CM et al (2013) Metabolic characteristics of castlemans disease on 18F-FDG PET in relation to clinical implication. *Clin Nucl Med* 38:339–342
39. Barker R, Kazmi F, Stebbing J et al (2009) FDG-PET/CT imaging in the management of HIV-associated multicentric Castlemans disease. *Eur J Nucl Med Mol Imaging* 36:648–652
40. Balamoutoff N, Serrano B, Hugonnet F, Garnier N, Paulmier B, Faraggi M (2018) Added value of a single fast 20-second deep-inspiration breath-hold acquisition in FDG PET/CT in the assessment of lung nodules. *Radiology* 286:260–270
41. Flavell RR, Behr SC, Mabray MC, Hernandez-Pampaloni M, Naeger DM (2016) Detecting pulmonary nodules in lung cancer patients using whole body FDG PET/CT, high-resolution lung reformat of FDG PET/CT, or diagnostic breath hold chest CT. *Acad Radiol* 23:1123–1129
42. Liu C, Alessio AM, Kinahan PE (2011) Respiratory motion correction for quantitative PET/CT using all detected events with internal-external motion correlation. *Med Phys* 38:2715–2723
43. B  ther F, Jones J, Seifert R, Stegger L, Schleyer P, Sch  fers M (2020) Clinical evaluation of a data-driven respiratory gating algorithm for whole-body PET with continuous bed motion. *J Nucl Med* 61:1520–1527
44. Kim JS, Lim ST, Jeong YJ, Kim DW, Jeong HJ, Sohn MH (2010) F-18 FDG PET/CT for the characterization of Castlemans disease according to clinical subtype. *J Nucl Med* 51:1614–1614
45. Rassouli N, Obmann VC, Sandhaus LM, Herrmann KA (2018) (18F)-FDG-PET/MRI of unicentric retroperitoneal Castlemans disease in a pediatric patient. *Clin Imaging* 50:175–180
46. H  ilund-Carlsen PF, Edenbrandt L, Alavi A (2019) Global disease score (GDS) is the name of the game! *Eur J Nucl Med Mol Imaging* 46:1768–1772
47. Raynor WY, Borja AJ, Rojulpote C, H  ilund-Carlsen PF, Alavi A. 18F-sodium fluoride: An emerging tracer to assess active vascular microcalcification. *J Nucl Cardiol*. 2020;
48. Boellaard R, Delgado-Bolton R, Oyen WJG et al (2015) FDG PET/CT: EANM procedure guidelines for tumour imaging: version 2.0. *Eur J Nucl Med Mol Imaging* 42:328–354
49. Graham MM, Wahl RL, Hoffman JM et al (2015) Summary of the UPICT protocol for 18F-FDG PET/CT imaging in oncology clinical trials. *J Nucl Med* 56:955–961
50. Ding Q, Zhang J, Yang L (2016) (18F)-FDG PET/CT in multicentric Castlemans disease: a case report. *Ann Transl Med* 4:58
51. Fu Z, Zhang X, Fan Y, Di L, Zhang J, Wang RF (2013) Clinical value of 18F-FDG PET/CT in the management of Castlemans disease. *J Nucl Med* 54:1560–1560
52. Murphy SP, Nathan MA, Karwal MW (1997) FDG-PET appearance of pelvic Castlemans disease. *J Nucl Med* 38:1211–1212
53. Haap M, Wiefels J, Horger M, Hoyer A, M  ssig K (2018) Clinical, laboratory and imaging findings in Castlemans disease—the subtype decides. *Blood Rev* 32:225–234
54. Mohammed A, Janku F, Qi M, Kurzrock R (2015) Castlemans disease and sarcoidosis, a rare association resulting in a “mixed” response: a case report. *J Med Case Rep* 9:45
55. Mohseni S, Shojaiefard A, Khorgami Z, Alnejad S, Ghorbani A, Ghafouri A (2014) Peripheral lymphadenopathy: approach and diagnostic tools. *Iran J Med Sci* 39:158–170
56. Wang W, Medeiros LJ (2019) Castlemans Disease. *Surg Pathol Clin* 12:849–863
57. Barua A, Vachlas K, Milton R, Thorpe JAC (2014) Castlemans disease- a diagnostic dilemma. *J Cardiothorac Surg* 9:170
58. Fajgenbaum DC, Langan R-A, Japp AS et al (2019) Identifying and targeting pathogenic PI3K/AKT/mTOR signaling in IL-6-blockade-refractory idiopathic multicentric Castlemans disease. *J Clin Invest* 129:4451–4463
59. Elboga U, Narin Y, Urhan M, Sahin E (2012) FDG PET/CT appearance of multicentric Castlemans disease mimicking lymphoma. *Rev Esp Med Nucl Imagen Mol* 31:142–144
60. Akosman C, Selcuk NA, Ordu C, Ercan S, Ekici ID, Oyan B (2011) Unicentric mixed variant Castlemans disease associated with Hashimoto disease: the role of PET/CT in staging and evaluating response to the treatment. *Cancer Imaging* 11:52–55
61. Casper C (2005) The aetiology and management of Castlemans disease at 50 years: translating pathophysiology to patient care. *Br J Haematol* 129:3–17
62. Ren N, Ding L, Jia E, Xue J (2018) Recurrence in unicentric castlemans disease postoperatively: a case report and literature review. *BMC Surg* 18:1
63. van Rhee F, Greenway A, Stone K (2018) Treatment of idiopathic Castlemans disease. *Hematol Oncol Clin North Am* 32:89–106
64. American Cancer Society. Castlemans Disease [Internet]. 2018 [cited 2020 Mar 15]. Available from: <https://www.cancer.org/cancer/castlemans-disease.html>
65. Pelosi E, Skanjeti A, Cistaro A, Arena V (2008) Fluorodeoxyglucose-positron emission tomography/computed tomography in the staging and evaluation of treatment response in a patient with Castlemans disease: a case report. *J Med Case Rep* 2:99
66. Jain L, Mackenzie S, Bomanji JB et al (2018) 18F-Fluorodeoxyglucose positron emission tomography-computed tomography imaging in HIV-infected patients with lymphadenopathy, with or without fever and/or splenomegaly. *Int J STD AIDS* 29:691–694
67. Di  val C, Bonnet DF, Maucl  re S et al (2007) Multicentric Castlemans disease: Use of HHV8 viral load monitoring and positron emission tomography during follow-up. *Leuk Lymphoma* 48:1881–1883
68. Sanz-Viedma S, Torigian DA, Parsons M, Basu S, Alavi A (2009) Potential clinical utility of dual time point FDG-PET for distinguishing benign from malignant lesions: implications for oncological imaging. *Rev Esp Med Nucl* 28:159–166
69. Borja A, Aly M, Seraj SM et al (2020) Role of FDG in the management of metastatic hepatic tumors treated with chemoembolization. *J Nucl Med Soc Nuclear Med* 61:1181–1181
70. Cheng G, Torigian DA, Zhuang H, Alavi A (2013) When should we recommend use of dual time-point and delayed time-point imaging techniques in FDG PET? *Eur J Nucl Med Mol Imaging* 40:779–787
71. Kwee TC, Basu S, Saboury B, Ambrosini V, Torigian DA, Alavi A (2011) A new dimension of FDG-PET interpretation: assessment of tumor biology. *Eur J Nucl Med Mol Imaging* 38:1158–1170
72. Sarikaya I, Sarikaya A (2020) Assessing PET parameters in oncologic 18F-FDG studies. *J Nucl Med Technol* 48:278–282
73. Kang F, Han Q, Zhou X et al (2020) Performance of the PET vascular activity score (PETVAS) for qualitative and quantitative assessment of inflammatory activity in Takayasu’s arteritis patients. *Eur J Nucl Med Mol Imaging* 47:3107–3117
74. Bai B, Bading J, Conti PS (2013) Tumor quantification in clinical positron emission tomography. *Theranostics* 3:787
75. Aide N, Lasnon C, Veit-Haibach P, Sera T, Sattler B, Boellaard R (2017) EANM/EARL harmonization strategies in PET quantification: from daily

- practice to multicentre oncological studies. *Eur J Nucl Med Mol Imaging* 44:17–31
76. Davis JC, Daw NC, Navid F et al (2018) 18F-FDG uptake during early adjuvant chemotherapy predicts histologic response in pediatric and young adult patients with osteosarcoma. *J Nucl Med* 59:25–30
  77. Im H-J, Zhang Y, Wu H et al (2018) Prognostic value of metabolic and volumetric parameters of FDG pet in pediatric osteosarcoma: a hypothesis-generating study. *Radiology* 287:303–312
  78. Basu S, Zaidi H, Salavati A, Hess S, Høiland-Carlsen PF, Alavi A (2014) FDG PET/CT methodology for evaluation of treatment response in lymphoma: from “graded visual analysis” and “semiquantitative SUVmax” to global disease burden assessment. *Eur J Nucl Med Mol Imaging* 41:2158–2160
  79. Taghvaei R, Zadeh MZ, Oestergaard B et al (2017) PET imaging in hematological malignancies. *J Nucl Med* 58:1008–1008
  80. Raynor WY, Zadeh MZ, Kotheekar E, Yellanki DP, Alavi A (2019) Evolving role of PET-based novel quantitative techniques in the management of hematological malignancies. *PET Clin* 14:331–340
  81. Borja AJ, Hancin EC, Zhang V, Revheim M-E, Alavi A (2020) Potential of PET/CT in assessing dementias with emphasis on cerebrovascular disorders. *Eur J Nucl Med Mol Imaging* 47:2493–2498
  82. Kotheekar E, Yellanki D, Borja AJ et al (2020) 18F-FDG-PET/CT in measuring volume and global metabolic activity of thigh muscles: a novel CT-based tissue segmentation methodology. *Nucl Med Commun* 41:162–168
  83. Borja AJ, Hancin EC, Dreyfuss AD et al (2020) 18F-FDG-PET/CT in the quantification of photon radiation therapy-induced vasculitis. *Am J Nucl Med Mol Imaging* 10:66–73
  84. Sun L, Sun X, Li Y, Xing L (2015) The role of (18)F-FDG PET/CT imaging in patient with malignant PEComa treated with mTOR inhibitor. *Oncotargets Ther* 8:1967–1970
  85. Graf N, Li Z, Herrmann K et al (2014) Positron emission tomographic monitoring of dual phosphatidylinositol-3-kinase and mTOR inhibition in anaplastic large cell lymphoma. *Oncotargets Ther* 7:789–798
  86. Owonikoko TK (2015) Inhibitors of mTOR pathway for cancer therapy, moving on from rapalogs to TORKinibs. *Cancer* 121:3390–3392
  87. Anwar H, Sachpekidis C, Schwarzbach M, Dimitrakopoulou-Strauss A (2017) Fluorine-18-FDG PET/CT in a patient with angiomyolipoma: response to mammalian target of rapamycin inhibitor therapy. *Hell J Nucl Med* 20:169–171

### Publisher's Note

Springer Nature remains neutral with regard to jurisdictional claims in published maps and institutional affiliations.

Submit your manuscript to a SpringerOpen<sup>®</sup> journal and benefit from:

- Convenient online submission
- Rigorous peer review
- Open access: articles freely available online
- High visibility within the field
- Retaining the copyright to your article

---

Submit your next manuscript at ► [springeropen.com](https://www.springeropen.com)

---